Polymer 50 (2009) 2510–2515

Contents lists available at ScienceDirect

Polymer

journal homepage: www.elsevier.com/locate/polymer

Thermal fractionation and effect of comonomer distribution on the crystal structure of ethylene–propylene copolymers

Zi-Xiu Du [a], Jun-Ting Xu [a,b,*], Qi Dong [a], Zhi-Qiang Fan [a,b]

[a] Key Laboratory of Macromolecular Synthesis and Functionalization, Department of Polymer Science and Engineering, Zhejiang University, Hangzhou 310027, China
[b] State Key Laboratory of Chemical Engineering, College of Materials and Chemical Engineering, Zhejiang University, Hangzhou 310027, China

ARTICLE INFO

Article history:
Received 18 June 2008
Received in revised form
26 March 2009
Accepted 4 April 2009
Available online 12 April 2009

Keywords:
Crystallization
Ethylene–propylene copolymer
Thermal fractionation

ABSTRACT

In this paper the comonomer distributions of two series of ethylene–propylene copolymers with different propylene contents, which were prepared by a fluorinated bis(phenoxyimine) Ti catalyst (FI–EP copolymers) and a conventional Ziegler–Natta catalyst (ZN–EP copolymers), respectively, were characterized. It is found that the comonomer distribution of ethylene–propylene copolymers can still be characterized by thermal fractionation at a long scale, though the propylene units can be incorporated into the PE crystal lattice. The FI–EP copolymers exhibit a narrow and random comonomer distribution, whereas a broad comonomer distribution is observed for the ZN–EP copolymers. The crystal structures of the FI–EP and ZN–EP copolymers were studied by WAXD. The *a*-axis of the PE crystals of the FI–EP copolymers increases rapidly with propylene content, indicating that more propylene units are incorporated into the PE crystal lattice, whereas only a slight expansion in *a*-axis is observed for the ZN–EP copolymers. WAXD result also shows the presence of hexagonal phase in the FI–EP copolymers and the relative content of the hexagonal phase increases with the propylene content, while in the ZN–EP copolymers the hexagonal phase is negligible.

1. Introduction

For the ethylene copolymers with a non-uniform comonomer distribution, there exist ethylene sequences of different lengths. These ethylene sequences have different crystallizabilities and may segregate upon crystallization [1,2], thus crystallization kinetics, morphology and mechanical properties are affected [3–6]. Comonomer distribution of ethylene–α-olefin copolymers can be characterized at different length scales. The structural heterogeneity at the scale of ~1 nm can be probed by ^{13}C NMR, since the chemical shift is usually affected by the adjacent five atoms [7]. Thermal fractionation is also used to characterize the comonomer distribution of ethylene–α-olefin copolymers, in which ethylene sequences of different lengths form discrete crystal populations of different lamellar thicknesses [8–13]. Assuming that all the comonomer units are excluded from the PE crystal lattice, the lamellar thickness of the PE crystals can be correlated with the length of the ethylene sequences [14–16]. Since only long sequences are involved in crystallization, thermal fractionation characterizes ethylene sequences of the length from several nanometers to tens of nanometers. To characterize comonomer distribution at a longer scale, combination of pyrolysis and fractionation is used [17].

Although characterization of sequence distribution at a short scale by ^{13}C NMR has been well reported for various ethylene–propylene copolymers, characterization of comonomer distribution at a long scale and its effect on crystallization behavior are rarely reported [18,19], as compared with other ethylene–α-olefin copolymers. The major difference between ethylene–propylene copolymer and other ethylene–α-olefin copolymers lies in that the methyl branches in the ethylene–propylene copolymer are less bulky and can be incorporated into the PE crystal lattice more readily, leading to expansion of the PE unit cell [20–25] and formation of hexagonal phase [26,27]. Such a unique characteristic of ethylene–propylene copolymer raises two questions, which have not been addressed in previous literature. Firstly, can thermal fractionation still be used to characterize comonomer distribution of ethylene–propylene copolymer at a long scale? Due to the incorporation of the methyl branches into the PE crystal lattice, the lamellar thickness of the PE crystals cannot be correlated with the length of the ethylene sequences in the ethylene–propylene copolymer. Secondly, does comonomer distribution affect crystal structure of ethylene–propylene copolymers? Since incorporation of the methyl branches

* Corresponding author. Key Laboratory of Macromolecular Synthesis and Functionalization, Department of Polymer Science and Engineering, Zhejiang University, 38 Zheda Road, Hangzhou 310027, Zhejiang Province, China. Tel./fax: +86 571 87952400.
E-mail address: xujt@zju.edu.cn (J.-T. Xu).

0032-3861/$ – see front matter © 2009 Elsevier Ltd. All rights reserved.
doi:10.1016/j.polymer.2009.04.006

inevitably creates voids in the PE crystal lattice, it may become disrupted when a large amount of propylene units are included. As a result, for an ethylene–propylene copolymer with a non-uniform comonomer distribution, it is expected that not all propylene units are incorporated into the PE crystal lattice and the incorporation of propylene units may depend on the local propylene content along the polymer chains. This means that the comonomer distribution may have an influence on the incorporation of propylene units into the PE crystal lattice.

For ethylene–α-olefin copolymers, the microstructures of copolymers produced by metallocene and Ziegler–Natta catalysts are frequently compared to reveal the effect of structure on properties, since it is generally believed that the active species in metallocene catalysts are "single site" and the prepared copolymers have a homogeneous comonomer distribution. However, the commonly used cocatalyst methylaluminoxane (MAO) for metallocenes is indeed a mixture, which may lead to a slight difference among the active species complexed with different MAO molecules [28,29]. Recently, it is found that fluorinated bis(phenoxyimine) Ti complex (FI catalyst), a new type of non-metallocene single site catalyst, can catalyze living polymerization of ethylene and propylene even though MAO is used as cocatalyst [30–33]. This means that the active species of this type of catalyst are homogeneous, and the obtained copolymers have a narrow molecular weight distribution and a random comonomer distribution. Therefore, ethylene–propylene copolymers prepared from FI catalyst are more suitable to be used as a reference than the metallocene-based copolymers. Here we characterized the comonomer distribution of ethylene–propylene copolymers prepared from the FI catalyst by thermal fractionation and compared with that of the ethylene–propylene copolymers prepared by a conventional Ziegler–Natta catalyst. The effect of comonomer distribution on crystal structure of ethylene–propylene copolymers was also reported.

2. Experimental

2.1. Synthesis and characterization of the ethylene–propylene copolymers

Copolymerization of ethylene and propylene catalyzed by a fluorinated bis(phenoxyimine) Ti (FI) catalyst was described elsewhere [34]. Copolymerization was carried out at 25 °C under atmospheric pressure in a 100-mL glass reactor equipped with a propeller-like stirrer and thermostat water bath. Toluene (50 mL) was introduced into the nitrogen-purged reactor and stirred (600 rpm), then the ethylene/propylene mixed gases were rapidly bubbled through the reactor. The flow rates of ethylene and propylene were regulated to levels that are much larger than the monomer consumption rate during the polymerization, so the monomer concentrations in the solution can be kept at a constant level. After 10 min, polymerization was initiated by adding a toluene solution of MAO (1.0 M, 4.0 mL) and then a toluene solution of catalyst (10 mM, 1.0 mL) into the reactor with stirring. Polymerization was terminated by addition of *sec*-butyl alcohol (10 mL), followed by introduction of ethanol (250 mL) and concentrated HCl (2 mL). The polymer was collected by filtration, washed with ethanol (200 mL), and dried in vacuum at 80 °C overnight. Copolymers with various propylene contents were prepared by changing the flow rates of ethylene and propylene.

Ethylene–propylene copolymers were also prepared by a conventional Ziegler–Natta (ZN) catalyst in a similar way. The catalyst is $TiCl_4/MgCl_2/SiO_2$/di-butyl phthalate with a Ti content of 3.0 wt%. The concentration of the ZN catalyst was 0.5 mg/mL. The cocatalyst was $AlEt_3$ (Al/Ti = 150) and dimethoxy diphenyl silane was used as external donor (Si/Ti = 7.5).

Molecular weight and molecular weight distribution of the ethylene–propylene copolymers were measured by GPC in a PL 220 GPC instrument (Polymer Laboratories Ltd.) at 150 °C in 1,2,4-trichlorobenzene. Three PL mixed-B columns (500–107) were used. Universal calibration against narrow polystyrene standards was adopted. Quantitative ^{13}C NMR spectra were recorded on a Varian Mercury 300-plus spectrometer at 120 °C in 10% (w/v) solution of *o*-$C_6D_4Cl_2$. $Cr(acac)_3$ was used to reduce the relaxation time of carbon atoms and the delay time was set as 3 s. The pulse angle was 90°, and 8000 scans were collected. The molecular weight, molecular weight distribution and propylene content are listed in Table 1. The ethylene–propylene copolymers prepared by the FI and ZN catalysts are denoted as FI–EP and ZN–EP copolymers, respectively.

2.2. Thermal fractionation

The polymer (about 6 mg) was sealed in an aluminum pan, which was put into a glass tube at argon atmosphere. The glass tube was immersed in an oil bath and heated to 180 °C, kept for 30 min, and then stepwise crystallized at 140 °C, 130 °C, 120 °C, 110 °C, 100 °C, 90 °C, 80 °C, 70 °C, 60 °C, 50 °C and 40 °C respectively, each for 12 h.

2.3. Differential scanning calorimetry (DSC)

DSC analysis was performed on a Perkin–Elmer Pyris-1 DSC calorimeter. The samples after thermal fractionation (stepwise crystallization) were scanned from 50 to 200 °C at a heating rate of 10 °C/min. For non-isothermal crystallization, the samples were heated to 160 °C and held for 5 min and then cooled to 50 °C at a rate of 10 °C/min. Heat flow during the cooling process was recorded.

2.4. Wide-angle X-ray diffraction (WAXD)

Wide-angle X-ray diffraction (WAXD) experiments were carried out on a Rigaku D/max 2550 PC with a Ni filtered Cu Kα radiation ($\lambda = 0.1546$ nm) at room temperature. The scan rate was 4° (2θ)/min at a step of 0.2°. Powder samples were used for WAXD test and stepwise crystallization was applied to the samples prior to WAXD experiments.

3. Results and discussion

3.1. Comonomer distribution of FI–EP and ZN–EP copolymers

Fig. 1 shows the DSC melting traces of ZN–EP copolymers after thermal fractionation. For the purpose of comparison, the DSC melting traces of FI–EP copolymers are also given, though they have been reported in our previous work [34]. Like other ethylene–α-olefin copolymers [35], multiple melting peaks are observed, which

Table 1
Molecular weight, molecular weight distribution and propylene content for FI–EP and ZN–EP copolymers.

Samples	*E*/*P* feed ratio (mL/min)	M_w ($\times 10^{-3}$)	M_w/M_n	[P] (mol%)
FI–EP0	300/0	239.7	1.29	0
FI–EP1	600/300	76.5	1.27	2.12
FI–EP2	300/60	17.11	1.27	5.09
FI–EP3	300/150	16.55	1.25	8.08
FI–EP4	300/300	13.25	1.19	11.40
FI–EP5	300/600	11.57	1.16	14.93
ZN–EP1	400/30	247.3	28.1	2.40
ZN–EP2	400/40	410.1	46.6	5.55
ZN–EP3	300/40	339.3	39.0	8.00
ZN–EP4	300/100	366.5	24.6	11.62
ZN–EP5	150/50	186.9	25.6	14.76

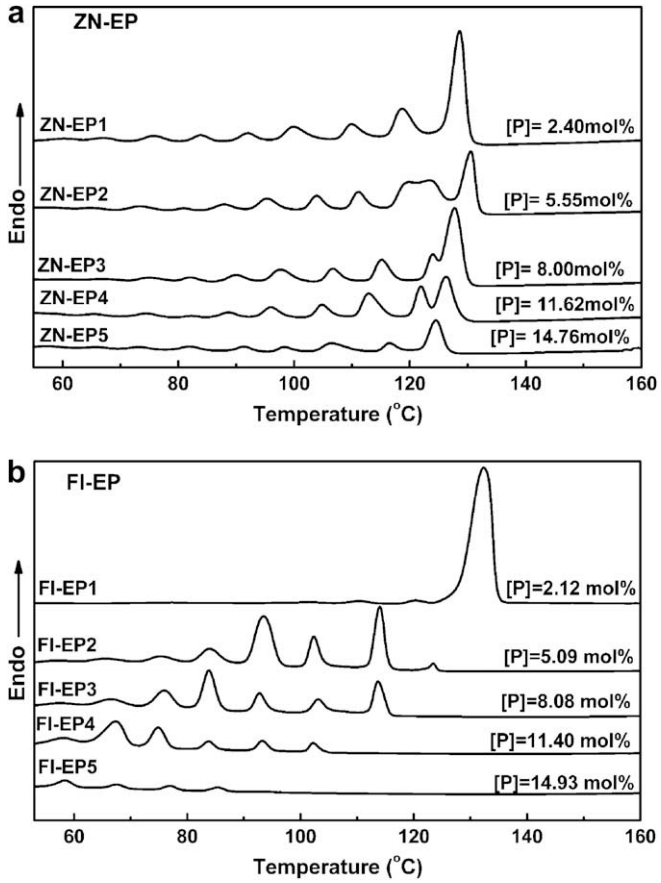

Fig. 1. DSC melting traces of the ZN–EP (a) and FI–EP (b) copolymers after stepwise crystallization.

correspond to the melting of PE crystals with different lamellar thicknesses. The appearance of multiple melting peaks is certainly related to the comonomer distribution. We believe that incorporation of the propylene units into the PE crystal lattice is dependent on the local propylene content in the polymer chains. If the local propylene content is low, the segment is crystallizable and the propylene units are incorporated into the PE crystal lattice. On the contrary, when the local propylene content is high, the segment is non-crystallizable and the propylene units are excluded from the PE crystal lattice. Here there is a difference between the ethylene–propylene copolymer and other ethylene–α-olefin copolymers. In the other ethylene–α-olefin copolymers, if the comonomer units are excluded from the PE crystal lattice, the lamellar thickness of PE crystals can be correlated with the length of ethylene sequences [14–16]. In contrast, for ethylene–propylene copolymer, the propylene units can be incorporated into the PE crystal lattice, thus the lamellar thickness of the PE crystals is related to the length of the crystalline (lower local propylene content) segments, which are longer than the ethylene sequences. Comparing with the melting traces of FI–EP and ZN–EP copolymers, there exist two striking differences. Firstly, for the ZN–EP copolymers the largest melting peak is always located at the highest temperature, irrespective of the propylene content, while for the FI–EP copolymers, the largest melting peak moves toward the middle with increasing propylene content. This shows that the longest crystalline segments, which form the thickest crystals and the highest melting temperature, are the majority in all the ZN–EP copolymers, while the crystalline segments with an intermediate length are the most in the FI–EP copolymers. The length of the crystalline segments is strongly dependent on the comonomer distribution. If the comonomer is randomly distributed, i.e. the enchainment of the comonomer units obeys Markovian model, the crystalline segments with an intermediate length are the most probable. However, when the comonomer is heterogeneously distributed in the same polymer chains or among different polymer chains, the amount of the longest crystalline segments and the amorphous segments will be abnormally large. This has been verified by both theoretical simulation and fractionation characterization [2,36]. Secondly, for the FI–EP copolymers the melting peaks at high temperature disappear gradually as the propylene content increases, whereas the highest melting peak exists in all the ZN–EP copolymers and does not change much with the propylene content. This leads to more melting peaks for the ZN–EP copolymers, especially at higher propylene content, indicating that the ZN–EP copolymers have a broader distribution of crystalline segments than the corresponding FI–EP copolymers. Moreover, the second difference shows that the longest crystalline segments in the ZN–EP copolymers are longer than those in the FI–EP copolymers, and the length and propylene content of these crystalline segments in the ZN–EP copolymers barely change with the overall propylene content, but the length gradually becomes shorter and the propylene content of the longest crystalline segments increases as the overall propylene content in the FI–EP copolymers. This can be further confirmed by the non-isothermal crystallization. Fig. 2 shows the change of crystallization temperature with propylene content for the FI–EP and ZN–EP copolymers. It is found that the crystallization temperature of the FI–EP copolymers decreases rapidly as the propylene content increases. In contrast, the crystallization temperature of the ZN–EP copolymers varies in a limited range (4 °C). Since the crystallization temperature is mainly determined by the segments of the strongest crystallizability, this result also shows that the length of the longest crystalline segments almost does not change with propylene content in the ZN–EP copolymers, but it decreases with propylene content in the FI–EP copolymers.

As revealed by DSC, the length and composition of the longest crystalline segments with the highest melting temperature in the ZN–EP copolymers hardly change with increasing the overall propylene content. As a result, we can deduce that, with increasing the overall propylene content, more and more propylene units are enchained in the amorphous segments with high local propylene content in the ZN–EP copolymers. This can be verified by ^{13}C NMR. Fig. 3 shows the ^{13}C NMR spectrum of ZN–EP4, which has a propylene

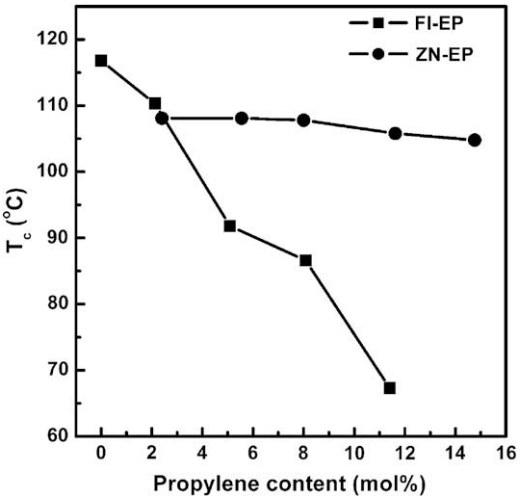

Fig. 2. Change of crystallization temperature with propylene content for the FI–EP and ZN–EP copolymers.

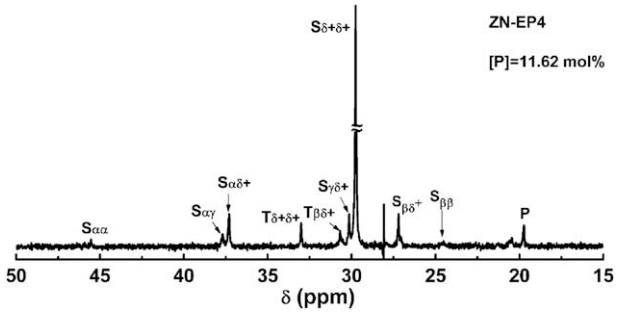

Fig. 3. ^{13}C NMR spectrum of ZN-EP4 with propylene content [P] = 11.62 mol%.

content [P] = 11.62 mol%. The appearance of $S_{\alpha\alpha}$ resonance at $\delta = 46.5$ ppm indicates the presence of continuous propylene unit, i.e. [PP] dyad, in this copolymer. There are more [PP] dyads in the ZN–EP copolymer with propylene content [P] = 14.76 mol%. Nevertheless, we did not observe [PP] dyad even in the FI–EP copolymer with propylene content [P] = 14.93 mol% (FI–EP5) [34].

Above results show that thermal fractionation can still be used to characterize comonomer distribution of ethylene–propylene copolymers at a long scale. The FI–EP copolymers have a random and narrower comonomer distribution, similar to the ethylene copolymers prepared by the single-site metallocene catalysts. In contrast, the ZN–EP copolymers have a more heterogeneous comonomer distribution. Moreover, considering the nature of plural active centers for the conventional heterogeneous Ziegler–Natta catalysts [37–39] and the broad molecular weight distributions of the ZN–EP copolymers, it is highly likely that the comonomer distributions among different polymer chains are quite different as well.

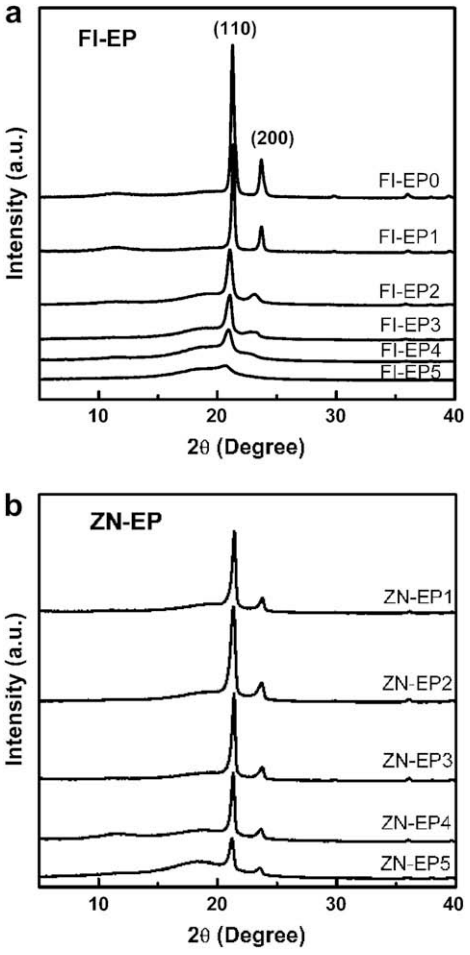

Fig. 4. WAXD patterns of FI–EP (a) and ZN–EP (b) copolymers after stepwise crystallization.

3.2. WAXD results

The WAXD patterns of the FI–EP and ZN–EP copolymers after stepwise crystallization are shown in Fig. 4. Two peaks appear at $2\theta = 21.2°$ and $2\theta = 23.7°$, which correspond to the (110) and (200) reflections of the orthorhombic PE crystals, respectively. Fig. 5 shows the crystallinity of FI–EP and ZN–EP copolymers calculated from WAXD using following equation [40]:

$$w_c = \frac{A_{(110)} + 1.42A_{(200)}}{A_{(110)} + 1.42A_{(200)} + 0.65A_a} \times 100\% \quad (1)$$

where $A_{(110)}$, $A_{(200)}$ and A_a are the areas of (110) reflection, (200) reflection and amorphous halo, which are obtained by fitting the WAXD profiles with Lorentzian function.

It is found that the crystallinity of the FI–EP copolymers changes in a wider range (from 63% to 27%) when the propylene content increases from 2.12 mol% to 14.93 mol%, but in the similar range of propylene content the crystallinity of the ZN–EP copolymers only changes from 55% to 38%. The FI–EP copolymers have larger crystallinity than the ZN–EP copolymers at lower propylene content level, but smaller crystallinity at higher propylene content level. This shows that propylene content has a greater influence on crystallinity in the FI–EP copolymers than in the ZN–EP copolymers. Such a difference originates from their different comonomer distributions. At lower propylene content, the presence of more non-crystalline segments leads to the smaller crystallinity of the ZN–EP copolymers than the FI–EP copolymers, and at higher propylene content, the presence of more crystalline segments with the highest melting temperature leads to the larger crystallinity of the ZN–EP copolymers than the FI–EP copolymers.

In Fig. 4 the positions of the reflections also change with the propylene content, especially for the (200) reflection. For orthorhombic PE crystal, the dimensions of the unit cell can be calculated according to the following equations:

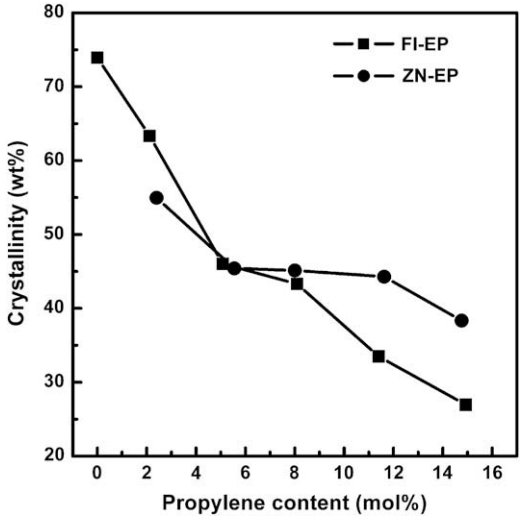

Fig. 5. Crystallinity of the FI–EP and ZN–EP copolymers measured by WAXD after stepwise crystallization.

$$a = 2d_{(200)} \quad (2)$$

$$b = \sqrt{a^2 d^2_{(110)}/a^2 - d^2_{(110)}} \quad (3)$$

where $d_{(200)}$ and $d_{(110)}$ are the distances of (200) and (110) crystalline planes, respectively, which can be calculated from Bragg equation. The parameters a and b are the dimensions of the a-axis and b-axis of the PE unit cell.

The variations of a and b with propylene content are shown in Fig. 6. It is found that the b-axis hardly changes with propylene content for both FI–EP and ZN–EP copolymers, which is in accordance with previous reports [20]. The dimension of a-axis increases slightly with propylene content for the ZN–EP copolymers, but it increases rapidly with propylene content for the FI–EP copolymers. The change of a-axis is an indicator for the amount of methyl branch incorporated into the PE crystal lattice. The more the methyl branches incorporated, the more obvious the expansion of the crystal lattice. The data in Fig. 6 show that the amount of methyl incorporated into the PE crystal lattice in the FI–EP copolymers is far larger than that in the ZN–EP copolymers, indicating that comonomer distribution has an important influence on the incorporation of methyl branches into the PE crystal lattice.

To facilitate discussion, we can convert the effect of comonomer distribution into the effect of comonomer content by assuming that

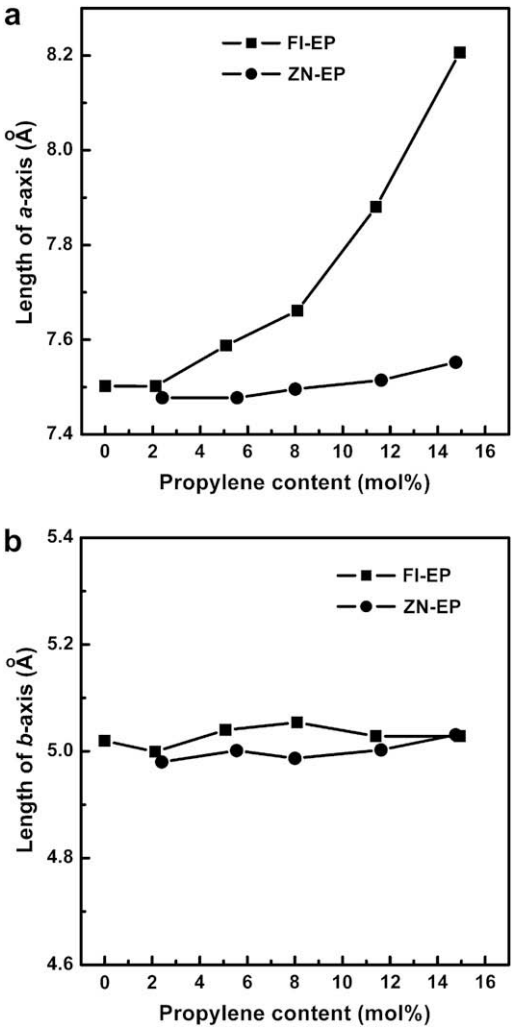

Fig. 6. Change of the lengths of a-axis (a) and b-axis of PE crystals as a function of propylene content.

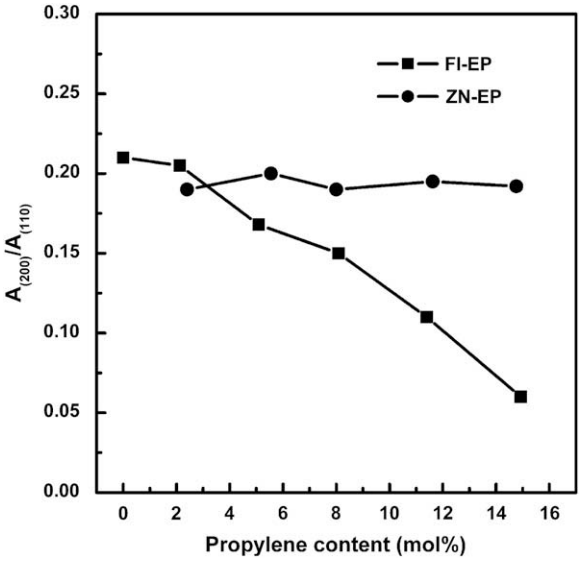

Fig. 7. The area ratios between (200) and (110) reflections ($A_{(200)}/A_{(110)}$) for the FI–EP and ZN–EP copolymers.

the comonomer units are uniformly distributed along the polymer chains. At low comonomer content, the methyl can be readily incorporated into the PE crystal lattice, since the PE crystal lattice is less distorted. However, at high comonomer content, the ethylene sequences are shorter and have weaker crystallizability. Moreover, incorporation of a larger amount of methyl may lead to serious distortion of the PE crystal lattice. At very high propylene content level the ethylene–propylene copolymer becomes even amorphous due to disruption of the PE crystals. As a result, only when the propylene content is limited in a suitable range, can the methyl branches be incorporated into the PE crystal lattice. When the propylene content exceeds a certain level, the polymer chains become amorphous and methyl branches are excluded from the PE crystal lattice. Since in the ZN–EP copolymers the crystalline segments with the highest melting temperature are the most, the local propylene content in the crystalline segments of the ZN–EP copolymers is smaller than that in the FI–EP copolymers at high level of overall propylene content. Therefore, fewer methyl branches are incorporated into the PE crystal lattice in the ZN–EP copolymers, resulting in a smaller expansion of a-axis. On the other hand, the crystalline segments of the FI–EP copolymers contain more propylene units, which can be incorporated into the PE crystal lattice, leading to a more obvious expansion of a-axis.

The data in Fig. 6 have shown that the incorporation of methyl can lead to the expansion of the PE unit cell. It has been proposed that, when a is equal to $b\sqrt{3}$, the orthorhombic unit cell happens to have hexagonal symmetry and "(pseudo)hexagonal" phase is formed [27]. But others believe that the hexagonal phase is a discrete phase different from the orthorhombic phase in symmetry [25]. Since in WAXD pattern the (100) reflection of hexagonal crystal is overlapped with the (110) reflection of orthorhombic crystal, it is difficult to quantitatively evaluate the relative content of hexagonal crystal by WAXD. Nevertheless, the presence of hexagonal phase will induce a decrease of the area ratio between (200) and (110) reflections ($A_{(200)}/A_{(110)}$), thus the content of hexagonal phase can be indirectly evaluated by comparison of the $A_{(200)}/A_{(110)}$ values of the neat polyethylene and the ethylene–propylene copolymers. Fig. 7 shows the variation of $A_{(200)}/A_{(110)}$ with propylene content for the FI–EP and ZN–EP copolymers. It is found that $A_{(200)}/A_{(110)}$ of the FI–EP copolymers decreases gradually as the propylene content increases, indicating that in FI–EP

copolymers the content of hexagonal phase increases with propylene content. In contrast, it is basically constant for all the ZN–EP copolymers, showing that the contents of the hexagonal phase in the different ZN–EP copolymers are similar. One can also see from Fig. 7 that the values of $A_{(200)}/A_{(110)}$ for the ZN–EP copolymers are close to those for the neat PE (FI–EP0) and FI–EP1 with propylene content of 2.12 mol%, implying that the content of the hexagonal phase in the ZN–EP copolymers is very low.

4. Conclusions

The results show that thermal fractionation still can be used to characterize comonomer distribution of ethylene–propylene copolymers at a long scale in spite of the incorporation of propylene units into the PE crystal lattice. It is found that the FI–EP copolymers have a random and narrower comonomer distribution, while the ZN–EP copolymers exhibit a more heterogeneous comonomer distribution. As revealed by WAXD, the amount of propylene units incorporated into the PE crystal lattice and the relative content of the hexagonal phase increase gradually with the propylene content in the copolymers for the FI–EP copolymers. In contrast, for the ZN–EP copolymers, the amount of propylene units incorporated into the PE crystal lattice barely changes with the overall propylene content and the content of the hexagonal phase is negligible. These differences can be attributed to their different comonomer distributions. Since the mechanical properties of EP copolymers are strongly dependent on the crystalline phase [27], the different comonomer distributions may also lead to different mechanical properties of the ZN–EP and FI–EP copolymers.

Acknowledgement

This work was supported by National Basic Research Program of China (2005CB623804) and State Key Laboratory of Chemical Engineering.

Appendix. Supplementary data

Supplementary data associated with this article can be found, in the online version, at doi:10.1016/j.polymer.2009.04.006.

References

[1] Hu WB, Mathot VBF. Macromolecules 2004;37:673.
[2] Hu WB, Mathot VBF, Frenkel D. Macromolecules 2003;36:2165.
[3] Fu Q, Chiu FC, McCreight KW, Guo MM, Tseng WW, Cheng SZD, et al. J Macromol Sci Phys 1997;B36:41.
[4] Zhang FJ, Liu JP, Xie FC, Fu Q, He TB. J Polym Sci Part B Polym Phys 2002;40:822.
[5] Zhang FJ, Song M, Lu TJ, Liu JP, He TB. Polymer 2002;43:1453.
[6] Wang MT, Bernard GM, Wasylishen RE, Choi P. Macromolecules 2007;40:6594.
[7] Carman CJ, Harrington RA, Wilkes CE. Macromolecules 1977;10:536.
[8] Starck P. Polym Int 1996;40:111.
[9] Chiu FC, Wang Q, Fu Q, Honigfort P, Cheng SZD, Hsiao BS, et al. J Macromol Sci Phys 2000;B39:317.
[10] Arnal ML, Balsamo V, Ronca G, Sanchez A, Muller AJ, Canizales E, et al. J Therm Anal Calorim 2000;59:451.
[11] Shanks RA, Amarasinghe G. J Therm Anal Calorim 2000;59:471.
[12] Starck P, Rajanen K, Lofgren B. Thermochim Acta 2003;395:169.
[13] Bialek M, Czaja K, Sacher-Majewska B. Thermochim Acta 2005;429:149.
[14] Zhang FJ, Liu JP, Fu Q, Huang HY, Hu ZJ, Yao S, et al. J Polym Sci Part B Polym Phys 2002;40:813.
[15] Zhang FJ, Fu Q, Lu TJ, Huang HY, He TB. Polymer 2002;43:1031.
[16] Xu JT, Xu XR, Feng LX. Eur Polym J 2000;36:685.
[17] Strate GV, Cozewith C, Ju S. Macromolecules 1988;21:3360.
[18] Zhang MZ, Duhamel J. Macromolecules 2007;40:661.
[19] Wright KJ, Lesser AJ. Macromolecules 2001;34:3626.
[20] Bassi IW, Corradini P, Fagherazzi GAV. Eur Polym J 1970;6:709.
[21] Shirayama K, Kita S, Watabe H. Makromol Chem 1972;151:97.
[22] Pérez E, Vanderhart DL. J Polym Sci Part B Polym Phys 1987;25:1637.
[23] Hosoda S, Nomura H, Gotoh Y, Kihara H. Polymer 1990;31:1999.
[24] Bracco S, Comotti A, Simonutti R, Camurati I, Sozzani P. Macromolecules 2002;35:1677.
[25] Hu WG, Srinivas S, Sirota EB. Macromolecules 2002;35:5013.
[26] de Ballesteros OR, Auriemma F, Guerra G, Corradini P. Macromolecules 1996;29:7141.
[27] Guerra G, De Ballesteros OR, Venditto V, Galimberti M, Sartori F, Pucciariello R. J Polym Sci Part B Polym Phys 1999;37:1095.
[28] Zurek E, Ziegler T. Prog Polym Sci 2004;29:107.
[29] Wang Q, Weng JH, Xu L, Fan ZQ, Feng LX. Polymer 1999;40:1863.
[30] Saito J, Mitani M, Mohri J, Yoshida Y, Matsui S, Ishii S, et al. Angew Chem Int Ed 2001;40:2918.
[31] Mitani M, Mohri J, Yoshida Y, Saito J, Ishii S, Tsuru K, et al. J Am Chem Soc 2002;124:3327.
[32] Tian J, Hustad PD, Coates GW. J Am Chem Soc 2001;123:5134.
[33] Hustad PD, Tian J, Coates GW. J Am Chem Soc 2002;124:3614.
[34] Du ZX, Xu JT, Wang X, Fan ZQ. Polym Bull 2007;58:903.
[35] Hsieh ET, Tso CC, Byers JD, Johnson TW, Fu Q, Cheng SZD. J Macromol Sci Phys 1997;36:615.
[36] Baker AME, Windle AH. Polymer 2001;42:651.
[37] Xu JT, Yang YQ, Feng LX, Kong XM, Yang SL. J Appl Polym Sci 1996;62:727.
[38] Xu JT, Feng LX, Yang SL, Yang YQ, Kong XM. Macromolecules 1997;30:7655.
[39] Xu JT, Feng JX, Yang SL, Yang YQ, Kong XM. Eur Polym J 1998;34:431.
[40] Mo ZS. Chin Polym Bull 1992;(1):26.